*Int. J. Solids Structures*, 1972, Vol. 8, pp. 261 to 267. Pergamon Press. Printed in Great Britain

# LONGITUDINAL IMPACT ON A CIRCULAR CYLINDRICAL TUBE

J. L. SACKMAN† and W. GOLDSMITH‡

University of California, Berkeley, California

**Abstract**—The longitudinal strain histories produced by impact in a long circular cylindrical tube are determined using membrane shell theory. Solutions are generated by a method which reformulates the boundary value problem in terms of Volterra integral equations which are then numerically resolved. The predicted histories are compared with strain histories measured in a corresponding experiment, and the correlation is found to be better than that based on histories predicted from elementary rod theory corrected to account for lateral inertia.

## INTRODUCTION

IN A recent paper, Goldsmith *et al.* [1] investigated the propagating strain pulses produced by longitudinal impact on a long circular cylindrical tube. Measurements were made of the longitudinal strain histories at five different stations along the tube resulting from the first passage of the pulse down the cylinder. These experimental data were then compared to theoretical predictions of the strain histories. The predictions were obtained by considering a close fit of the data at the station nearest the impacted end of the tube to be the prescribed input, and then calculating the resulting output at the four downrange stations. These calculations were based on elementary rod theory, corrected to account for lateral inertia according to the procedure given by Rayleigh. The correlation obtained between the experimental data and the theoretical predictions was, in general, good. However, there remained discrepancies which could not be relegated to experimental or computational error, but which were probably due to deficiencies in the mathematical model used to describe the wave propagation phenomenon resulting from impact. To effect an improvement in the correlation between the data and theoretical predictions, it would appear necessary to utilize a more refined theory than that employed in [1]. In this paper we investigate the consequences of employing membrane shell theory to model the behavior of the tube by comparing the predictions of the longitudinal strain histories at the four downrange stations based on that theory to those which were actually measured there, as reported in [1]. We obtain the predicted strain histories by using a calculational procedure based on a convenient method of analysis of pulse propagation problems which employs Volterra integral equations.

† Professor of Engineering Science.
‡ Professor of Applied Mechanics.

## ANALYSIS

According to membrane shell theory, the equations governing the axially symmetric motion of a circular cylindrical tube are

$$\frac{\partial \sigma_z}{\partial z} = \rho \frac{\partial^2 u_z}{\partial t^2}; \qquad \frac{\sigma_\theta}{R} = \rho \frac{\partial^2 u_r}{\partial t^2}$$

$$\varepsilon_z = \frac{\partial u_z}{\partial z}; \qquad \varepsilon_\theta = \frac{u_r}{R} \tag{1}$$

$$\sigma_z = \frac{E}{1-\nu^2}(\varepsilon_z + \nu\varepsilon_\theta); \qquad \sigma_\theta = \frac{E}{1-\nu^2}(\varepsilon_\theta + \nu\varepsilon_z)$$

where, in the usual notation, $u$, $\varepsilon$ and $\sigma$ represent, respectively, the displacement strain and stress, $z$ the coordinate along the axis of the shell, $r$ and $\theta$ the polar coordinates in the plane of the circular cross-section of the shell and $t$ the time. The radius of the shell is signified by $R$, $\rho$ is the density of the shell material and $E$ and $\nu$ are, respectively, Young's modulus and Poisson's ratio of the shell material.

The Laplace transform of the longitudinal strain at any station $z$ in the tube is obtained as

$$\bar{\varepsilon}_z(z, p) = \bar{\varepsilon}_z(0, p)\bar{f}(z, p) \tag{2}$$

where $\varepsilon_z(0, t)$ is the longitudinal strain at $z = 0$, and

$$\bar{f}(z, p) = \exp\left[-p/c\sqrt{\left(\frac{p^2+\alpha^2}{p^2+\beta^2}\right)}z\right] \tag{3}$$

$$\alpha = c/R, \qquad \beta = \sqrt{(1-\nu^2)}\alpha. \tag{4}$$

The signal velocity in the tube is given by

$$c = \sqrt{[E/\rho(1-\nu^2)]}. \tag{5}$$

Here we are concerned only with the solution which represents the first passage of the pulse down the tube. In the above we have used a superposed bar to indicate the Laplace transform of a function with respect to the time variable, with $p$ representing the transform parameter.

To invert equation (2), we begin by noting that we can rewrite $\bar{f}$ as

$$\bar{f} = e^{-pz/c}\bar{h}(z, p) \tag{6}$$

where

$$\bar{h}(z, p) = e^{-(pz/c)\bar{g}} \tag{7}$$

with

$$1 + \bar{g} = \sqrt{\left(\frac{p^2+\alpha^2}{p^2+\beta^2}\right)}. \tag{8}$$

By squaring equation (8) and inverting we obtain

$$2g(t)+\int_0^t g(t-\tau)g(\tau)\,\mathrm{d}\tau = \frac{\alpha v^2}{\sqrt{(1-v^2)}}\sin\beta t. \tag{9}$$

This nonlinear Volterra integral equation of the second kind can be inverted readily by numerical means to yield the function $g(t)$.

From the properties of the exponential we see that

$$\bar{h}(z,p) = 1+\bar{h}_R(z,p) \tag{10}$$

where

$$\bar{h}_R(z,p) = \frac{h_R(z,0)}{p}+\frac{\dot{h}_R(z,0)}{p^2}+\cdots \tag{11}$$

with

$$h_R(z,0) = -cv^2z/R^2. \tag{12}$$

A superposed dot is used to represent differentiation with respect to time. If now we differentiate equation (7) with respect to the transform parameter $p$, we obtain

$$\frac{\partial\bar{h}_R(z,p)}{\partial p} = -\frac{z}{c}\frac{\mathrm{d}}{\mathrm{d}p}[p\bar{g}(p)]\bar{h}(z,p). \tag{13}$$

This equation can be inverted into the time domain to give the Volterra integral equation of the third kind

$$th_R(z,t)+\frac{z}{c}\int_0^t \tau\dot{g}(\tau)h_R(z,t-\tau)\,\mathrm{d}\tau = -zt\dot{g}(t)/c. \tag{14}$$

Having $g(t)$ from the resolution of (9) and knowing $h_R(z,0)$ from (12), equation (14) is easily resolved numerically to obtain the function $h_R(z,t)$ for any choice of $z$. With $h_R(z,t)$ in hand we may now solve for the longitudinal strain $\varepsilon_z(z,t)$ by combining equations (2), (6) and (10). The result is

$$\varepsilon_z(z,t) = \varepsilon^*\left(z, t-\frac{z}{c}\right) \tag{15}$$

where

$$\varepsilon^*(z,t) = \varepsilon_z(0,t)+\int_0^t \varepsilon_z(0,t-\tau)h_R(z,\tau)\,\mathrm{d}\tau. \tag{16}$$

In summary, the inversion of equation (2) is performed by first obtaining $g(t)$ from a numerical resolution of (9). Then, using equation (12), equation (14) is numerically resolved to obtain $h_R(z,t)$ for the value of $z$ of interest. Next the convolution integral in equation (16) is numerically evaluated to yield $\varepsilon^*(z,t)$. Finally $\varepsilon_z(z,t)$ is obtained from equation (15).

For later discussion it is convenient to also have the hoop strain $\varepsilon_\theta(z,t)$. It may be obtained from equation (1) in terms of the longitudinal strain. The result is

$$\varepsilon_\theta(z,t) = -\alpha v\int_0^t \varepsilon_z(z,\tau)\sin\alpha(t-\tau)\,\mathrm{d}\tau. \tag{17}$$

## DISCUSSION

The way we used the data of Ref. [1] was to consider a close fit of the measured longitudinal strain at the station nearest the impact end (hereafter denoted as the base station) as prescribing the function $\varepsilon_z(0, t)$ (see Fig. 1). With this known input history we used the preceding analysis to predict the strain $\varepsilon_z(z, t)$ at each of the downrange stations located a distance $z$ from the base station (the corresponding values of $z$ were $z = 20$, 40, 60 and 80 in.) and then compared these results with the strains actually measured at these stations. These comparisons are given in Figs. 2–5. The measured strain history at the base station

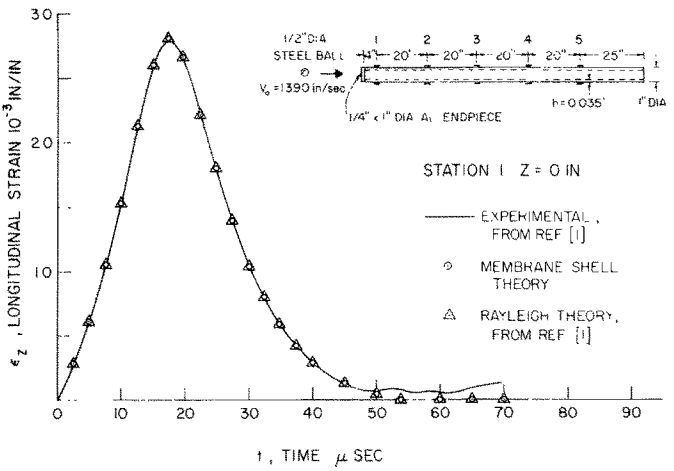


FIG. 1. Theoretical and experimental longitudinal strain–time curves for a straight tube due to concentric longitudinal impact by a $\frac{1}{2}$ in. diameter steel sphere at an initial velocity of 1390 in./sec. Station 1, $z = 0$ in.

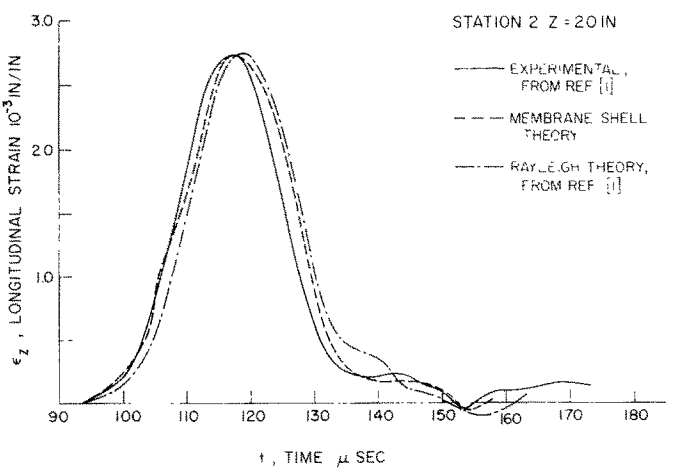


FIG. 2. Theoretical and experimental longitudinal strain–time curves for a straight tube due to concentric longitudinal impact by a $\frac{1}{2}$ in. diameter steel sphere at an initial velocity of 1390 in./sec. Station 2, $z = 20$ in.

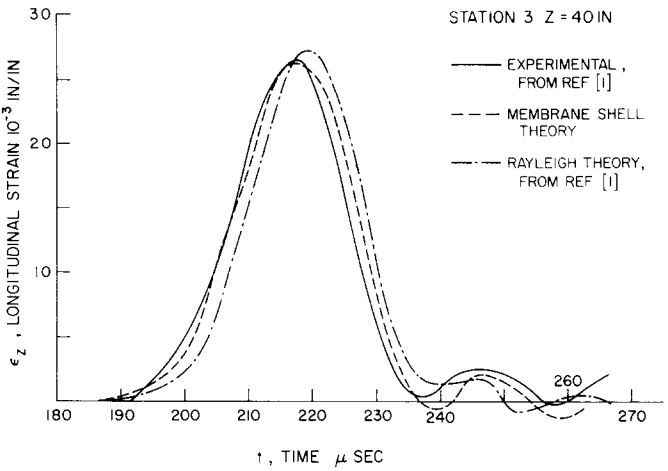


FIG. 3. Theoretical and experimental longitudinal strain–time curves for a straight tube due to concentric longitudinal impact by a $\frac{1}{2}$ in. diameter steel sphere at an initial velocity of 1390 in./sec. Station 3, $z = 40$ in.

is given in Fig. 1, along with the approximation of it (denoted in the figure as "Theory") which we used in our computation of the theoretical predictions at the four downrange stations.

The outer diameter and wall thickness of the tube used in the experiment were 1 and 0·035 in., respectively. The mechanical properties of the 2024 aluminum used in our computations were: density = 0·100 lb/in.$^3$, $\nu = 0{\cdot}322$ and $c = 0{\cdot}2145$ in./$\mu$ sec. We took for $R$ (to be used in the membrane shell theory) the value of $\frac{1}{2}$ in. Our choice of $\nu$ and $c$ was obtained from some numerical experimentation based on an attempt to optimize the correlation between the predicted and measured longitudinal strain histories.

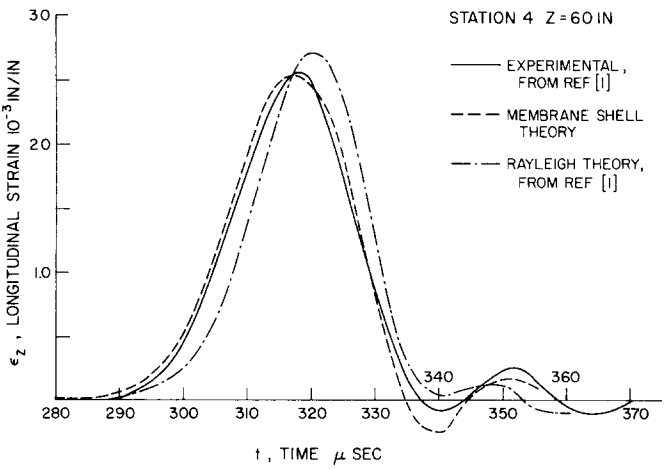


FIG. 4. Theoretical and experimental longitudinal strain–time curves for a straight tube due to concentric longitudinal impact by a $\frac{1}{2}$ in. diameter steel sphere at an initial velocity of 1390 in./sec. Station 4, $z = 60$ in.

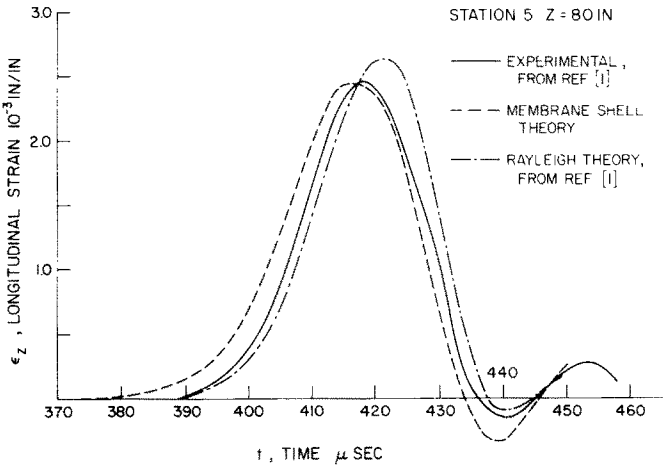


FIG. 5. Theoretical and experimental longitudinal strain–time curves for a straight tube due to concentric longitudinal impact by a $\frac{1}{2}$ in. diameter steel sphere at an initial velocity of 1390 in./sec. Station 5, $z = 8$ in.

It may be seen from the figures that at all four downrange stations the correlation between the experimental results and the theoretical predictions based on membrane shell theory is quite good. These results represent an improvement over the correlation obtained when the theoretical predictions were based on elementary rod theory including Rayleigh's correction for lateral inertia. As a check on our numerical computation, we also calculated the response histories by numerically solving the partial differential equations (1) using the method of characteristics. Within plotting accuracy, no discernible differences between the two sets of computed values were noted.

After calculating $\varepsilon_z(z, t)$, we next used equation (17) to compute the hoop strain history $\varepsilon_\theta(z, t)$. The results obtained were interesting. At each station, the hoop strain history had a shape almost identical to the longitudinal strain history. However, the ratio of the maximum value of $\varepsilon_\theta$ to that of $\varepsilon_z$ at each station was always larger than Poisson's ratio and decreased as $z$ increased. For the particular example considered in Figs. 2–5 this ratio for $z = 20, 40, 60$ and 80 in. was approximately 0·38, 0·37, 0·36 and 0·35, respectively. This computed behavior is in accord with the phenomenon actually observed in the experiments reported in [1].

In closing, we note that we also computed the longitudinal strain history $\varepsilon_z(z, t)$ corresponding to a step function input [i.e. for $\varepsilon_z(0, t) = H(t)$, where $H(t)$ is the Heaviside step function]. It is interesting to observe that for large values of $z$, the rich structure of this computed history was very similar in form to the longitudinal stress history caused by a constant velocity impact of a circular cylindrical tube against a rigid obstacle as reported by Berkowitz [2] for stations far from the impact end. He obtained his solution (also based on membrane shell theory) by the use of integral transforms and approximate inversions carried out by means of asymptotic methods.

*Acknowledgments*—The authors are grateful to F. Jourdan, H. Penicaud and C. L. Wu for writing the computer program and performing the numerical computations.

## REFERENCES

[1] W. GOLDSMITH, P. LEE and J. L. SACKMAN, Pulse propagation in straight circular elastic tubes. *J. appl. Mech.* in press.
[2] H. M. BERKOWITZ, Longitudinal impact of a semi-infinite elastic cylindrical shell. *J. appl. Mech.* **30**, 347–354 (1963).

(*Received* 23 *April* 1971; *revised* 9 *July* 1971)

**Абстракт**—Пользуясь теорией безмоментных оболочек, определяются истории цеформаций удлинения, вызванных ударом по длинной, круглой, цилиндрической трубе. Обобщаются решения методом преобразовывающим задачи краевого условия в выражениях интегральных уравнений Вольтеррц, которые, затем решаются численно. Сравниваются предусматриваемые истории с историями деформации, измеренными в соотвуствующем опыте. Получается лучшая сходимость чем основанной на историях вытекающих из элементарной теории стержня, уточненной учетом поверхностной инерции.